UNIVERSIDADE
EDUARDO
MONDLANE

ESCOLA SUPERIOR DE CIÊNCIAS MARINHAS E COSTEIRAS

Dissertation presented in partial fulfilment of the requirements for the Master Degree in Applied Oceanography

INVESTIGATING THE CURRENTS STRUCTURE IN THE NORTHERN MOZAMBIQUE CHANNEL, CABO - DELGADO

Author:

Adelina António Langa

Quelimane, February 2025

UNIVERSIDADE
E D U A R D O
MONDLANE

ESCOLA SUPERIOR DE CIÊNCIAS MARINHAS E COSTEIRAS

Dissertation presented in partial fulfilment of the requirements for the Master Degree in Applied Oceanography

Investigating the Currents Structure in the Northern Mozambique Channel, Cabo - Delgado

Chairman of the jury

Dr. Avelino A. A. Langa
UEM-Escola Superior de Ciências Marinhas e Costeiras

Supervisor:

Professor Doutor Tor Gammelsrød
Bergen University – Geophysical Institute

Co-Supervisor:

Prof. Doutor Hélder Machaieie
UEM-Escola Superior de Ciências Marinhas e Costeiras

Examiner:

Professor Doutor Øyvind Breivik
Norwegian Meteorological Institute

Quelimane, February 2025

"Eu não procuro saber as respostas, procuro compreender as perguntas"

(Confúcio)

Acknowledgements

First of all, I would like to thank God for the gift of life.

Secondly, I would like to thank my supervisors Professor Doutor Tor Gammelsrød, Prof. Doutor Helder Machaieie and Professor Doutor Antonio Mubango Hoguane for their tireless support throughout my journey.

I sincerely want to thank the entire EAF-Nansen Programme team for their support in acquiring the data.

"This research uses data collected through scientific surveys with the research vessel *Dr Fridtjof Nansen* as part of the collaboration between the Food and Agriculture Organization of the United Nations (FAO) on behalf of the EAF-Nansen Programme and the Republic of Mozambique. The EAF-Nansen programme in partnership between the FAO, the Norwegian Agency for Development Cooperation (Norad), and the Institute of Marine Research (IMR) in Norway for sustainable management of fisheries in partner countries and regions".

I am pleased to have shared this time with all the other master's students of the Escola Superior de Ciencias Marinhas e Costeiras – Universidade Eduardo Mondlane, especially the Applied Oceanography class of 2022. I want to extend my thanks, especially to my colleague and friend Nélio das Neves for his support, and friendship during our journey.

My thanks also go to Professors Avelino Langa and Anildo Naftal for their tireless support during this journey.

And without forgetting my family (Mom & Dad I love you so much, my lovely siblings, my adorable little niece & nephew) and close friends who have always believed in me.

Declaration

I declare that this dissertation has never been submitted for any degree and consists of the result of my individual labour originally written by me, with the full support of my supervisors. This dissertation is presented in partial fulfilment of the requirements for the degree of Master's in Applied Oceanography at Eduardo Mondlane University.

Signature

(Adelina António Langa)

Abstract

The Northern Mozambique Channel has been an area of interest for several marine operations in the prospecting and exploiting of offshore hydrocarbons. Thus, a detailed understanding of the local circulation and dynamics is crucial for safety and environmental monitoring in case of an oil spill event. In the present study, a combination of different data set products was used to infer the structure of the currents and the related processes that affect their variability in the Northern Mozambique Channel. We used CTD and ADCP measurements data collected during the research cruise ship "*Dr Fridtjof Nansen"* in March 2018, and the satellite altimetry-derived geostrophic currents. A longitudinal transect was considered off Cabo-Delgado, Quissanga district - 12 ºS with almost 100 km distance, we concentrated on the upper 200 m depth where we have ADCP measurements. Our results presented three different modes of the current structure from a horizontal perspective: on the coastal tip, the currents are southwards orientated with moderate velocities of up to 0.6 m/s and vertically homogeneous, intensifying towards the sea at 1000 m isobaths with strong velocities of up to 1 m/s south-westwards orientated, while on the eastern part of the transect at around 2000 m isobaths, the near-surface currents (above 50 m depth) are completely weak (< 0.2 m/s) and are north-westwards orientated. The weak north-westwards currents at the near-surface (above 50 m depth) observed off 2000 m isobaths are wind-driven, with less influence from the Sea Surface Height gradient. The strong south-westerly currents are found to be a result of the Sea Surface Height gradient, and their intensity is affected by the rugged steering topography on the west coast of the Channel. Moreover, the Channel is dominated by anticyclonic eddies propagating southwards with current speeds (> 1 m/s). These results suggest the need for delicate and suitable materials and methods for offshore operations, as the floating platform installations will have to withstand very strong currents up to a depth of more than 1000 m. The current speeds are fast enough to move the spilt oil to the coast quickly, affecting the coastal ecosystems and consequently human health.

Keywords: currents structure, Northern Mozambique Channel, CTD, ADCP, Geostrophic currents, Sea Surface Height

Resumo

O Canal Norte de Moçambique tem sido uma área de interesse para várias operações marítimas na prospeção e exploração de hidrocarbonetos em mar aberto. A compreensão detalhada da circulação e dinâmica local é crucial para a segurança e monitorização ambiental em casos de derrame de petróleo. Neste estudo, foi utilizada a combinação de diferentes conjuntos de dados para inferir a estrutura das correntes e os processos relacionados a sua variabilidade no Norte do Canal de Moçambique. Foram utilizados dados colhidos pelos instrumentos CTD e ADCP durante o cruzeiro de investigação *"Dr. Fridtjof Nansen"*, conduzido em Março de 2018, e correntes geostróficas derivadas da altimetria de satélite. Foi considerado um transecto longitudinal ao largo de Cabo-Delgado, distrito de Quissanga - 12 ºS, com quase 100 km de distância, concentrou-se nos primeiros 200 m de profundidade onde temos medições ADCP. Os resultados apresentam três modos diferentes da estrutura da corrente numa perspetiva horizontal: na parte costeira, as correntes são orientadas para Sul com velocidades moderadas até 0,6 m/s e verticalmente homogéneas, intensificando-se em direção ao mar aberto nas isóbatas de 1000 m com fortes velocidades até 1 m/s orientadas para Sudoeste, enquanto que na extremidade oriental do transecto, em torno das isóbatas de 2000 m, as correntes de superfície (acima de 50 m de profundidade) são completamente fracas (< 0,2 m/s) e orientadas para Noroeste. As correntes fracas de Noroeste na superfície, observadas ao largo das isóbatas de 2000 m são impulsionadas pelo vento, com menor influência do gradiente da altura da superfície do mar. As correntes fortes de Sudoeste são resultantes do gradiente da altura da superfície do mar e a sua intensidade é afetada pela topografia acidentada da costa Oeste do Canal. Adicionalmente, o Canal é dominado por vórtices anticiclónicos que se propagam para Sul com velocidades de corrente (> 1 m/s). Estes resultados, sugerem a necessidade de materiais, métodos delicados e adequados para as operações em alto mar, uma vez que as instalações das plataformas flutuantes terão de suportar correntes muito fortes até uma profundidade superior a 1000 m. Estas velocidades são suficientemente rápidas para transportar o petróleo derramado para a costa, afetando os ecossistemas costeiros e, consequentemente, a saúde humana.

Palavras-Chave: Estrutura de corrente, Canal Norte de Moçambique, CTD, ADCP, correntes geostróficas, altura da superfície do mar

List of Abbreviations and Acronyms

AC – *Agulhas Current*

ACSEX *– Agulhas Current Source Experiment*

ADCP – *Acoustic Doppler Current Profiler*

CODAS – *Common Ocean Data Access System*

CTD – *Conductivity Temperature and Depth*

EACC – *East African Coastal Current*

ECMWF - *European Centre for Medium-Range Weather Forecasts*

FAO *– Food Agriculture Organization*

FLNG *– Floating Liquefied Natural Gas*

GEBCO – *General Bathymetry Chart of the Oceans*

GPS - *Geographical Position System*

LOCO *– Long-Term Ocean Climate Observation*

MC – *Mozambique Current*

NetCDF – *Network Common Data Format*

NMC – *Northern Mozambique Channel*

SEC – *South Equatorial Current*

SLA – *Sea Level Anomaly*

SSH *– Sea Surface Height*

List of Figures

List of Tables

Table of Contents

1 INTRODUCTION

The circulation in the Mozambique Channel is intense and dynamic with significant climate events. Due to its location between Madagascar and the coast of Africa, the circulation is driven mainly by the South Equatorial Current (SEC), which moves from the Northern tip of Madagascar toward mainland Africa where it bifurcates at, approximately, 10 °S, before described by Sætre and Da Silva, (1984). In addition to the narrow location of the Mozambique Channel, the main SEC source moves equatorward, resulting in the East African Coastal Current (EACC), and the other part moves inland, forming the Mozambique Current (MC) (Sætre, 1985).

These characteristics lead the Mozambique Channel to be dominated by cyclonic and anticyclonic eddies. Previous studies on the investigation of the circulation of the Mozambique channel (Sætre and Da Silva, 1984; Ruijter et al., 2002, 2004; Quartly and Srokosz, 2004; Harlander et al., 2009), stated that hydrographic observations have shown that the flow within the Mozambique Channel, is best described by a series of large inland-propagating anticyclonic eddies (diameters > 300 km) that propagate southward. The formation of these eddies occurs regularly and is related to the strength of the volume transport through the channel (Ruijter et al., 2002).

Ullgren et al., (2012), studying hydrography and proprieties of water mass in the Mozambique Channel found the same results, assuming that the events of current intensification may be related to eddies specifically anticyclones, when these eddies hit a western boundary, tend to propagate southward which may block the northward transport of the deep water mass and thus enhance the southward transport along the western slope of Channel. In-situ measured current structures of the eddy field in the Mozambique Channel Ternon et al., (2014) concluded that anticyclones features are generally the dominant structure within the eddy field.

Studying eddy structure, dynamic and current direction in the Northern Mozambique Channel Vassele, (2010), suggested that the currents can be considered to be in geostrophic equilibrium, and whereas these geostrophic currents are Westward intensified - Northern zone and Eastward intensified - Southern zone, having velocities of more than 1 m/s. These results can be reinforced by Ullgren et al., (2016), who observed strong ocean currents offshore Pemba, Northern Mozambique of about 1m/s on the surface and deep currents

approximately 1000 m depth maximum velocities as high as 0,6 m/s, which may be considered very strong for currents at this depth level.

Moving a little bit to the Centre area of the channel, Miramontes et al., (2019), studying the influence of bottom currents on the Zambezi Valley morphology a study based on in-situ current observations and hydrodynamic modelling, presented periods of intense currents at the seafloor with peaks of 0,4 m/s – 0,6 m/s that last up to one month.

Overall, these studies, indicate that the current was found to be aligned with the bottom topography, and the strongest current events were southward-westward. The other possibility is that the strong deep ocean currents are probably caused by warm anticyclone eddies interacting with the boundary nearby or formed locally by instabilities in the narrows of the Mozambique Channel. On the other hand, these strong bottom-current events are correlated with a change in current direction and an increase in temperature.

From previous studies, most of which used numerical models and long-term moorings it is possible to get a general overview of the circulation, dynamic and mesoscale processes that govern the Mozambique Channel. However, detailed information about the structure of current in the regional perspective combining different data sets products is scarce. To provide new insights in this field, we aim to: investigate the current structure and the processes that govern their variability in the Northern Mozambique Channel, Cabo-Delgado. We use observational CTD and ADCP data measured in-situ and altimetry-derived data such as Sea Surface Height and winds to investigate the structure of the currents (currents velocity, direction, magnitude and other crucial physical parameters) and the process that affects their variability.

1.1 Thesis organization

This master thesis is organized as follows:

(1) A brief introduction to the work is presented, the research questions followed by the objectives, and finally the motivation and relevance of the development of this research;
(2) This chapter presents a brief literature review that underpins the research, touching on the essential points about the circulation and dynamics of the Mozambique Channel;
(3) The data, instruments and main methods are presented in this chapter, with a brief introduction on how the data were acquired and processed by the different sources and *software*;
(4) The results and discussion of the in situ measurements and altimetry-derived observations are presented in this chapter;
(5) Key conclusions are presented;
(6) Appendixes with the step-by-step description of the use of the CODAS ADCP processing software and the deep CTD stations.

1.1.1 Research Questions

This research stands for the following research questions:

- What are the characteristics and structure of the currents in the Northern Mozambique Channel?

- What are the processes associated with the variability of the current structure in the Northern Mozambique Channel?

1.1.2 Objectives

Main Objective

The main objective of this research is to investigate the current structure in the Northern Mozambique Channel, Cabo-Delgado

Specific Objectives

For the success of this research, the following specific objectives were defined:

- Describe the current structure (velocity, direction, magnitude) in the Northern Mozambique Channel;

- Identify the processes that affect the variability of the current structure in the Northern Mozambique Channel.

1.1.3 Thesis Statement

The coast of Mozambique is rich in energy resources such as oil and natural gas, and in some regions hydrocarbon exploration and production has already begun, both onshore and offshore. Specifically in the Northern Mozambique Channel (Rovuma basin in Cabo-Delgado), offshore oil and gas exploration using a Floating Liquefied Natural Gas (FLNG) platform in area 4 - Coral Sul has already started with production. A second Floating Platform - Coral Norte - will be installed in the next few years, about 10 km North of the FLNG - Coral Sul (Instituto Nacional de Petroleo , 2023).

The Environmental Impact Assessment of these gas exploration and production activities in the Rovuma basin (Cabo–Delgado), suggests that no critical issues have been identified, namely unacceptable environmental and social risks that could affect the viability of the gas exploration and production project in Cabo Delgado, information shared by Consultec - an Environmental Consultancy Company (*JornalNacional_02.07.2023*). However, this Environmental Impact Assessment study does not extend to the investigation of oceanographic parameters. Oceanographic processes, such as local circulation, can potentially influence the magnitude of the consequences of accidents at work, including oil spills.

On the other hand, the circulation dynamics of the Northern Mozambique Channel are quite intense and complex, dominated by mesoscale vortices and the occurrence of extreme weather events such as cyclones and tropical storms. Many studies have been undertaken to investigate the dynamics and circulation in the Mozambique Channel due to its interesting characteristics. Some of these studies were addressed specifically to the eddy field (Backeberg and Reason, 2010; Vassele, 2010; Ternon et al., 2014) and the state of the bottom currents discussed by Ullgren et al., (2016) in the Northern Mozambique Channel.

Overall, most of the studies use a wide-ranging and enriched methodology that provides general overview information about the characteristics of circulation and dynamics in the Mozambique Channel. However, detailed studies that report on local circulation, the structure of currents and their dynamic variability using a combination of different data sets still require more attention.

Surface production platforms will have to withstand the forces of ocean currents at a depth of more than 1000 m isobaths, and a good knowledge of the local ocean current's structure regime and circulation dynamics is necessary to ensure the safe performance of offshore operations.

In this context, this research aims to focus on the investigation of the current structure in the northern region of the Mozambique Channel, Cabo-Delgado - Quissanga, to bring insights that can be useful to the scientific community, to engineers in the energy resources sector and the society, ensuring the sustainable exploitation and production of resources for the improvement of the blue economy in Mozambique.

2 BACKGROUND

2.1 The Circulation in the Mozambique Channel (From old to recent conceptual description)

The circulation in the Mozambique Channel has for many years attracted the attention of several scientists due to its specific and complex characteristics. This can be reinforced by the number of enriched oceanographic data of high spatial and temporal resolution that are measured in this region.

2.1.1 Old Conceptual Description of the Mozambique Channel

The Mozambique Current is usually considered a part of the anti-cyclonic sub-tropical gyre consisting of the South Equatorial Current, the Agulhas Current system and the eastward flow situated to the north of the sub-tropical convergence (Saetre and da Silva, 1982).

Based on a sparse dataset available to the oceanographic community, different portrayals of the oceanic surface circulation in the region have been proposed (Fig.1). Historical data, and old textbooks have suggested that the surface circulation in the channel was mainly dominated by a southward flowing, western boundary current along the Mozambican coastline, and known as the Mozambique Current (Sætre and Da Silva, 1984; Sætre, 1985; Donguy and Piton, 1991).

The water flowing southwards in the Mozambique Channel is mostly derived from the South Equatorial Current. The northern part of the Mozambique Current as well as its main source, the South Equatorial Current, is directly influenced by the monsoon winds (Saetre and da Silva, 1982).

The monsoons are characterized by seasonal changes in wind direction throughout the year, during the summer monsoon (September-March) North to North-East quadrant it is mainly characterized by tree anticyclonic cells, with the large one in the centre of the channel (Fig 1c). During the winter monsoon (April-August) South to South-West quadrant is dominated by a larger number of small-scale circulation cells (Fig 1d). However, considerable seasonal variations in velocity and volume transport are therefore to be expected.

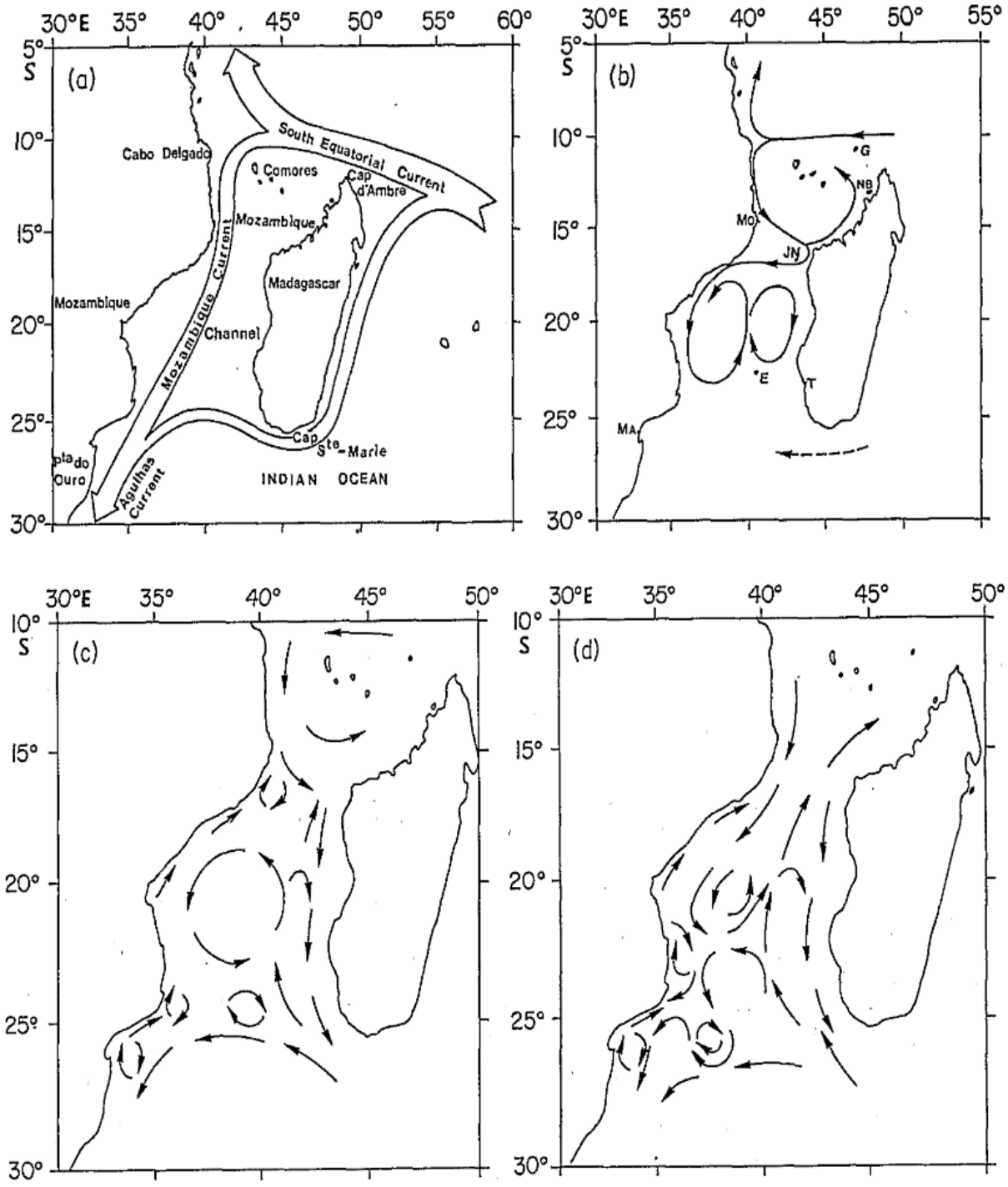

Figure 1. *Illustration of different diagrams proposed to characterize the nature of the flow in the Mozambique Channel. Panel (a) - proposed by Sætre, 1985, based on historical data. Panel (b) - proposed by Soares (1975), based on meteorological data, and tide Gauge stations. Panels (c: summer monsoon, d: winter monsoon) - proposed by Sætre and Da Silva, 1984, also [After: (Donguy and Piton, 1991)].*

2.1.2 Recent conceptual description of the Mozambique Channel

2.1.1.1 Mesoscale eddies and Currents

After the discoveries mentioned above in Chapter 2.1.1, some questions about the circulation pattern in the channel had no straightforward answers. Likely in recent years efforts have been made to make discoveries and enrich the existing information.

Investigating the nature and continuity of the Mozambique Current, hydrographic stations, at the narrow section of the Mozambique Channel by the Agulhas Current Source Experiment (ACSEX) cruise Ruijter et al., (2002) provided results that seem to close the debate about whether the flow in the channel was continuous or not. They observed that the flow in the Mozambique Channel is discontinuous and dominated by a train of large anti-cyclonic eddies (diameters > 300 km) that reach the channel bottom and propagate southward (Ridderinkhof and Ruijter, 2003; Ruijter et al., 2002).

Based on satellite altimeter observations combined with in situ observations from the ACSEX programme Schouten et al., (2003), studying eddies and variability in Mozambique Channel redefined the portrayal of the flow in the Mozambique Channel Figure 2.

Continuously, using a relatively larger dataset by the Long-Term Ocean Climate Observation (LOCO) moorings, also deployed at the narrow of the channel around 17 °S, as part of the Dutch LOCO programme which involves continuous currents, temperature and salinity observations over the full depth and width of the Channel, as well as altimetry remote sensing data also support the concept of a flow being dominated by a series of anticyclonic eddies (Harlander et al., 2009).

The word eddy, in the Mozambique Channel, is generally used to describe features with length scales falling in the range of tens and hundreds of kilometres in diameter, and with time scales of 10 - 30 days. These eddies can occur at a frequency of 4 - 7 per year they cause a net poleward transport of about 15 Sv (1 Sv = 10^6 m^3/s) (Ruijter et al., 2002).

Modelling studies suggest that eddies are formed by barotropic and baroclinic instabilities of the South Equatorial Current North of Madagascar, and propagate southward along the coast (Halo et al., 2013). These modelled eddies showed that are strong surface intensified and the amplitude in terms of vertical displacement of isopycnals can be 100 m or more, and the associated currents velocities can be higher than 1 m/s at the surface.

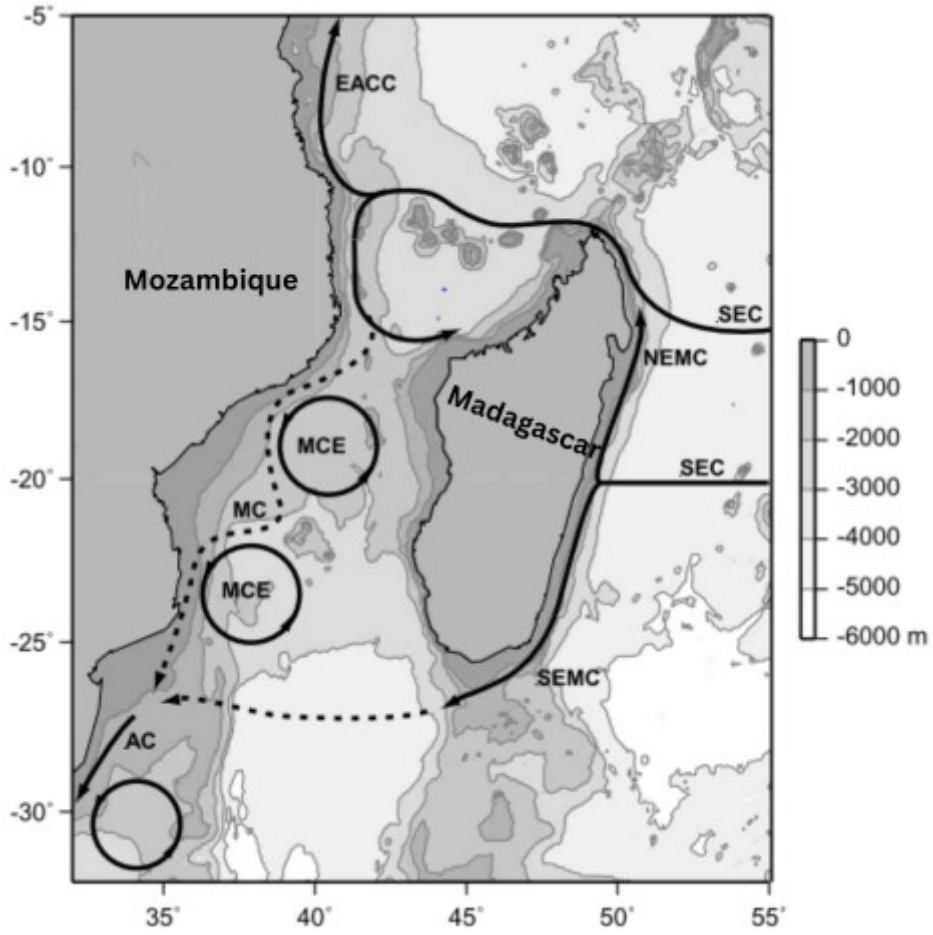

Figure 2. *Representation of the schematic main currents circulation and bathymetry of the Mozambique Channel. The Channel is limited by two countries: Mozambique in the West and Madagascar in the East. Features shown are the South Equatorial Current (SEC), the Northeast and Southeast Madagascar Currents (NEMS and SEMC), the East African Coastal Current (EACC), the Agulhas Current (AC), Mozambique Channel Eddies (MCE) and the Mozambique Current (MC). Source: (Schouten et al., 2003).*

Investigations of eddy occurrence frequency in the different regions of the channel show that in the Northern zone, eddies have been observed at a larger frequency of about 7 per year. In the Central region, they have a frequency of about 4 - 5 per year, while in the Southern region, they have been observed at a rate of 3 - 4 per year (Schouten et al., 2003).

The interesting fact is that these eddies propagate mostly south-westwards along the Mozambican coastline, inducing the current direction in this way.

3 DATA, INSTRUMENTS AND METHODS

This research focuses on the Northern zone of the Mozambique Channel, Cabo-Delgado, Quissanga District, as shown in Figure 3.

To investigate the current structure in the Northern Mozambique Channel (NMC), we used data from the research cruise ship *"Dr Fridtjof Nansen"* made available by the Food and Agriculture Organization of the United Nations (FAO) on behalf of the EAF-Nansen Programme and the Republic of Mozambique. It should be noted that all protocol was observed for the acquisition of the data, for more details see the "acknowledgements" chapter.

To describe the flow and structure of the currents (velocity, direction and magnitude), CTD (Conductivity Temperature and Depth) and ADCP (Acoustic Doppler Current Profiler) we used observed in situ data. These data were sectioned for the Northern zone specifically at latitude (-12 ^{o} S) where the longitudinal transect was built at approximately 40 ^{o} E to 42 ^{o} E, from March, 25 th and 26 th, 2018 considering 16 CTD stations and 161 ADCP files.

CTD stations and ADCP track from a depth of approximately 20 m of the sectioned area are scattered together as presented in Figure 3, together with the bathymetry of the respective sampled area which ranges from 200 m to 2500 m.

Additionally, we use satellite altimetry data derived from winds and Sea Surface Height (SSH), for the two-day measurements, to compare and validate the in situ observations and identify processes associated with the variability of current dynamics and structure.

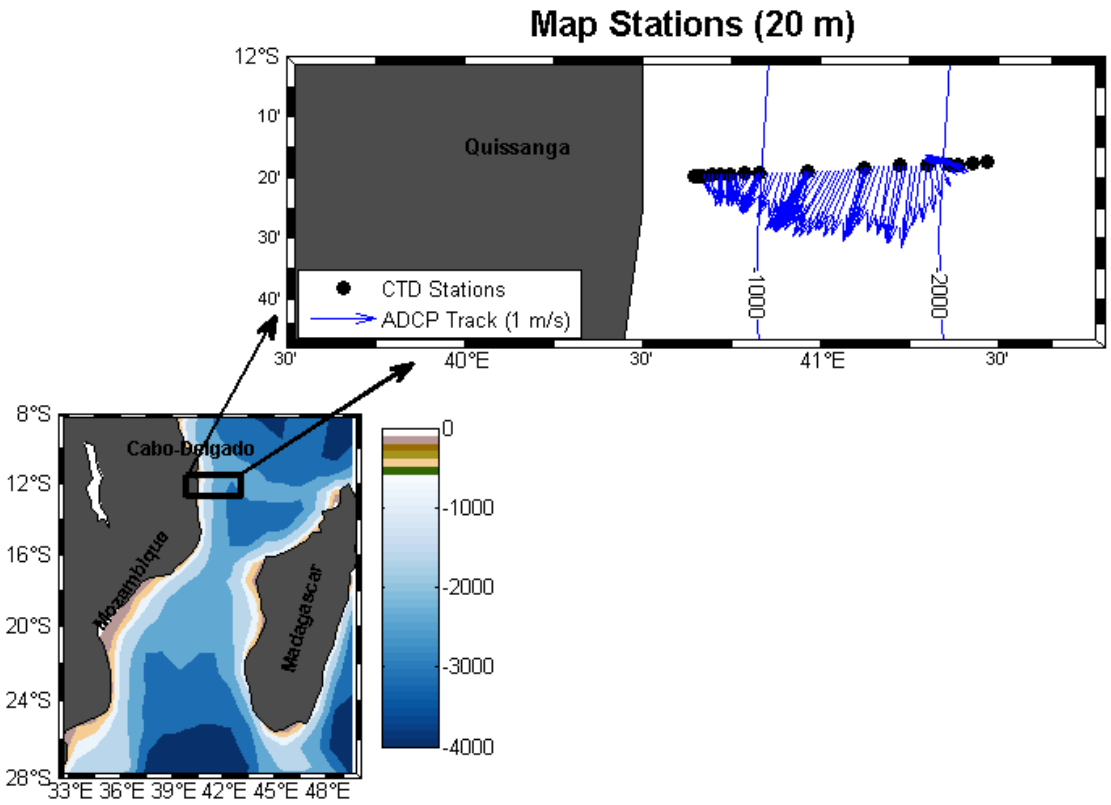

Figure 3. *Illustration of the study area. The bathymetric map of the Mozambique Channel with depths ranging from 200 m - 3500 m. The rectangle shows the sampling area with CTD stations (o) and ADCP track (arrow). Specifically for the sampled transect the depths* range from 200 m – 2500 m.

Table 1. *In-situ current measurement products*

Ship	Cruise ID	Instrument	depth m	Temporal resolution	Period
Dr. Fridtjof Nansen	km1001c_demo	ADCP	20 600	5’	25th.03.2018 26th.03.2018
		CTD	3 2000	N/A	25th.03.2018 26th.03.2018

Table 2. *Altimetry-derived current data*

Dataset	Product	Grid	Temporal resolution	Period
Copernicus Marine Service (https://doi.org/10.48670/moi-00148)	Sea Surface Height	1/4º	Daily	25th.03.2018 26 th.03.2018

Table 3. *Altimetry-derived wind data*

Dataset	Product	Grid	Temporal resolution	Period
Climate Copernicus (**https://cds.climate.copernicus.eu/cdsapp#!/dataset/reanalysis-era5-single-levels?tab=overview**)	Wind	1/4º	Hourly	25th.03.2018 26 th.03.2018

3.1 Sea Surface Height Data

Altimetry satellites measure the distance from the satellite to the ocean surface by recording the time it takes a radar pulse to make a round-trip from the satellite to the sea surface and back again (https://marine.copernicus.eu/).

The geostrophic currents field and the Sea Surface Height data from multiple altimeter missions are merged to provide a gridded map. In this study, we used reanalysis satellite altimetry data product available from Copernicus Marine Service, (https://doi.org/10.48670/moi-00148). The data correspond to a daily average gridded data with 0.25^{o} spatial resolution, where two data products were considered: Sea Surface Height above geoid and absolute dynamic topography and the absolute geostrophic velocities for the two components East (u) and North (v).

3.2 Wind Data

For the wind data, we used the recent ERA5 reanalysis dataset, produced by the European Centre for Medium-Range Weather Forecasts (ECMWF) for the two-day measurements. ERA5 is the fifth generation atmospheric reanalyses of the global climate and can be freely accessed from the Copernicus Climate Data Store (https://cds.climate.copernicus.eu/). The ERA5 replaces the ERA-Interim reanalyses, presenting considerable improvements, (horizontal dimension - 31 km, vertical dimension - 137 levels, and 1 h), the upgrade of the assimilation system and the radiative transfer model, the larger period covered, and the better representation of physical processes (Hersbach et al., 2020).

The sea surface wind speed data correspond to the latitude-longitude grid (0.25^{o}) and temporal resolution (hourly), for the two components: 10 m u-component wind and 10 m v-component wind.

3.3 In situ Measurements

3.3.1 Conductivity, Temperature and Depth (CTD) Data

The CTD is an instrument developed to determine seawater properties. The CTD instruments have collected high-resolution near-surface and deep Conductivity (which relates to the salinity) Temperature and Depth of ocean water (www.coml.org/investigating/measuring/ctds.html).

In this study, we used measurements obtained from the CTD - SBE 11plus V 5.2 version instrument. After acquiring the CTD data, the physical parameters such as temperature, salinity and pressure data were used to calculate the density (sigma-theta). Once the density in each depth layer is known, it is possible to calculate the geostrophic current in depth (z).

3.3.1.1 Geostrophic Velocity in Depth (z) Estimates

Geostrophic currents are an integral part of ocean currents at all depths and locations (Stewart, 2008). Under 100 m deep and about 100 km from the coast, all the currents are geostrophic; near the surface and close to contour boundaries they are modified by additional forces. Geostrophic currents establish the geostrophic balance, which is the balance between the pressure gradient force and the Coriolis force, and the velocity is perpendicular to the pressure gradient and Coriolis forces (Gammelsrød, 2008).

It is necessary to solve multiple equations to determine the geostrophic currents:

From the hydrostatic and Geostrophic surface currents,

$\partial p = -\rho g \partial z$; (eq. 1) $\quad v = \frac{1}{\rho f}\frac{\partial p}{\partial x}$; (eq. 2a) $\quad u = -\frac{1}{\rho f}\frac{\partial p}{\partial y}$; (eq. 2b)

The pressure is hydrostatic, given by equation (1). Then near the surface, the pressure is given by integrating the hydrostatic differential equation from the reference depth h_0 to the surface η, as follows:

$$\int_{z=p(ho)}^{z=p(\eta)} dp = -\int_{z=-h0}^{z=\eta} \rho g dz = -\rho g\,(\eta + h0\,);\ \text{(eq. 3)}$$

Substituting in equations (2), and given that h_0 is constant, we have the expressions for the geostrophic velocity at the surface which is a function of the horizontal gradient of the surface elevation.

$$v = \frac{1}{\rho f}\,\frac{\partial(-\rho g(\eta + h0\,))}{\partial x} = -\frac{g}{f}\,\frac{\partial \eta}{\partial x}\ ;\ \text{(eq. 4a)}$$

$$u = \frac{1}{\rho f}\,\frac{\partial(-\rho g(\eta + h0\,))}{\partial y} = \frac{g}{f}\,\frac{\partial \eta}{\partial y}\ ;\ \text{(eq. 4b)}$$

Assuming that the flow is hydrostatic, according to equation (1), and that *f* does not vary with depth, we have:

$$\frac{\partial(\rho v)}{\partial z} = -\frac{g}{f}\,\frac{\partial \rho}{\partial x}\ ;\ \text{(eq. 5a)} \qquad \frac{\partial(\rho u)}{\partial z} = \frac{g}{f}\,\frac{\partial \rho}{\partial y}\ ;\ \text{(eq. 5b)}$$

With Boussinesq's approximation, which states that the density variation is not important except in the pressure and lift terms, we have:

$$\frac{\partial v}{\partial z} = -\frac{g}{\rho f}\,\frac{\partial \rho}{\partial x}\ ;\ \text{(eq. 6a)} \qquad \frac{\partial u}{\partial z} = \frac{g}{\rho f}\,\frac{\partial \rho}{\partial y}\ ;\ \text{(eq. 6b)}$$

Equations (6) are called the thermal wind and are the geostrophic velocity equations. Once we know the density field at x and y, it is possible to calculate the density gradients.

If we know the current at a depth and the density field elsewhere, we can integrate $\frac{\partial u}{\partial z}$ and $\frac{\partial v}{\partial z}$ to determine the velocity components u(z) and v(z).

In this case, the geostrophic current velocity of the North component at a reference depth of 200 m was calculated in equation 7, assuming the reference z (200 m) = 0 we have the equation:

$$v(z) = -\frac{g}{\rho f}\int_{-200}^{z}\frac{\partial \rho}{\partial x}dz \quad \text{(eq. 7)}$$

To correct the null values (equal to zero) observed at 200 m depth in the CTD derived geostrophic currents, for each pair of CTD station there were calculated averages of corresponding ADCP measured currents in the section, as the CTD stations and ADCP section were aligned, see Figure 3.

3.3.2 Acoustic Doppler Current Profiler (ADCP) Data

The ADCP instrument transmits high-frequency acoustic signals which are backscattered from plankton, suspended sediment, and bubbles, all of which are assumed to be travelling with the mean speed of the water (Ternon et al., 2014). The ADCP estimates horizontal and vertical velocity as a function of depth by using the Doppler Effect to measure the radial relative velocity between the instrument and scatters in the ocean. (www.coml.org/investigating/measuring/adcps.html)

The ADCP instrument was mounted on the hull of research cruise "*Dr Fridtjof Nansen*" to 150 kHz RDI Ocean Surveyor I, with a time average of 5 min per ensemble and depth varying from 20 m to 600 m. We considered two days of measurements 25th and 26th, of March 2018, for the sampling area of our transect section.

The ADCP data was acquired in the form of a "row-data" version and was first pre-processed using the "CODAS (Common Ocean Data Access System) ADCP Processing" platform (currents.soest.hawaii.edu/docs/adcp_doc/codas_doc/introduction.html) refers to a suite of open-source programs for processing ADCP data.

The CODAS processing suite of programs consists of C and Python programs that will run on Windows, Linux, or Mac OSX, and process data collected from a Broadband or Ocean Surveyor data by VmDAS, or data collected by any of those instruments using UHDAS (open source acquisition software that runs RDI ADCPs) (currents.soest.hawaii.edu/docs/adcp_doc/codas_doc/introduction.html).

The CODAS database (Common Ocean Data Access System) is not a hierarchical database; it is a portable, self-descriptive file format (in the spirit of netCDF), that was designed specifically for ADCP (and other oceanographic) data. For historical reasons, it is stored as a collection of files. Because it is an organized body of information, it is referred to as a database. (currents.soest.hawaii.edu/docs/adcp_doc/codas_doc/introduction.html).

Following the pre-processing step-by-step using the CODAS platform, the netCDF (network common data format) file was compiled, making it possible to carry out the post-processing using the Matlab software (Math Works programming language) in the 2013a version.

4 RESULTS

This chapter presents the results for the oceanographic parameters: water masses, temperature, salinity and density. These parameters describe the physical characteristics of the circulation and are essential for calculating geostrophic currents in the depths presented later on. Relevant results are also presented for the direction, velocity and magnitude of currents in the North of the Mozambique Channel, Cabo-Delgado.

4.1 Physical parameters

4.1.1 Water Masses

A temperature versus salinity diagram or T-S diagram which relates density to the observed values of temperature and salinity are presented in figures 4(a) and 4(b), used to identify the water masses at the sectioned area 12 ºS latitude, around 40.7 ºE - 42 ºE longitude.

The T-S profile (Fig. 4a), presents the vertical profiles of temperature and salinity of one of the deepest stations (2000 m) in the transect, to get a better picture of the distribution of different water masses in depths in the T-S diagram (Fig. 4b). The relative maximum temperature value of up to 30 ºC is observed at the surface and decrease abruptly in the thermocline zone 10 ºC at 500 m. Below this zone, temperature gradually decreases to a minimum of 2 ºC at a maximum depth of 2000 metres. The amplitude of the salinity isoline indicates an increase of salinity with a relative maximum of up to 35.3 ‰ at the surface up to 300 m, below this depth there is an abrupt decrease to a relative minimum of up to 34.7 ‰ at 700 m, the 1000 m is marked by medium values of up to 34.9 ‰, followed by a slight decreasing of up to 34.78 ‰ at maximum depth 2000 m.

The T-S diagram (Fig. 4b) presents water masses with high-temperature values of approximately 30 ºC and low salinity values of roughly 34.8 ‰ at the surface. The temperature decreases as the depth increases, while the salinity increases to a maximum of 35.3‰ as the temperature decreases to an accessible 14 ºC - 13 ºC. Further down, the salinity decreases to its minimum peak of 34.7‰ at a temperature of 8 ºC, below this temperature, the salinity also presents low values.

The T-S curve (Fig. 4b), presents different water masses composed of Tropical Surface Water (TSW) at the surface, characterized by relatively warm waters ranging from temperatures 24 ºC - 28 ºC, low salinities 34.91‰ - 35.31‰ and low densities (sigma-theta)

are expected 22 - 24 kg.m^{-3}. This is a clear signal of the influence on the South Equatorial Current of surface water masses TSW, which has a relatively low salinity because of the excess precipitation and it contains Pacific water transported via the Indonesian through flow (Dimarco et al., 2002). The Subtropical Surface Water (STSW) in the subsurface 8 ºC – 25 ºC and 35.60‰ - 35.80‰ salinities, these results are in concordance with (Breitzke et al., 2017; Miramontes et al., 2019).

The permanent thermocline is mainly composed of South Indian Central Water (SICW) with temperatures ranging from 6 ºC - 16 ºC, the salinities range from 34,5‰ - 35,6‰. Deeply the Antarctic Intermediate Water (AAIW) with temperatures ranging from 2 ºC – 10 ºC, an interesting fact is the low salinities of 33.8‰ - 34.8‰. This can be supported by the fact of this water mass being diluted when entering into the South-West Indian Ocean via the Mozambique and Madagascar Basins.

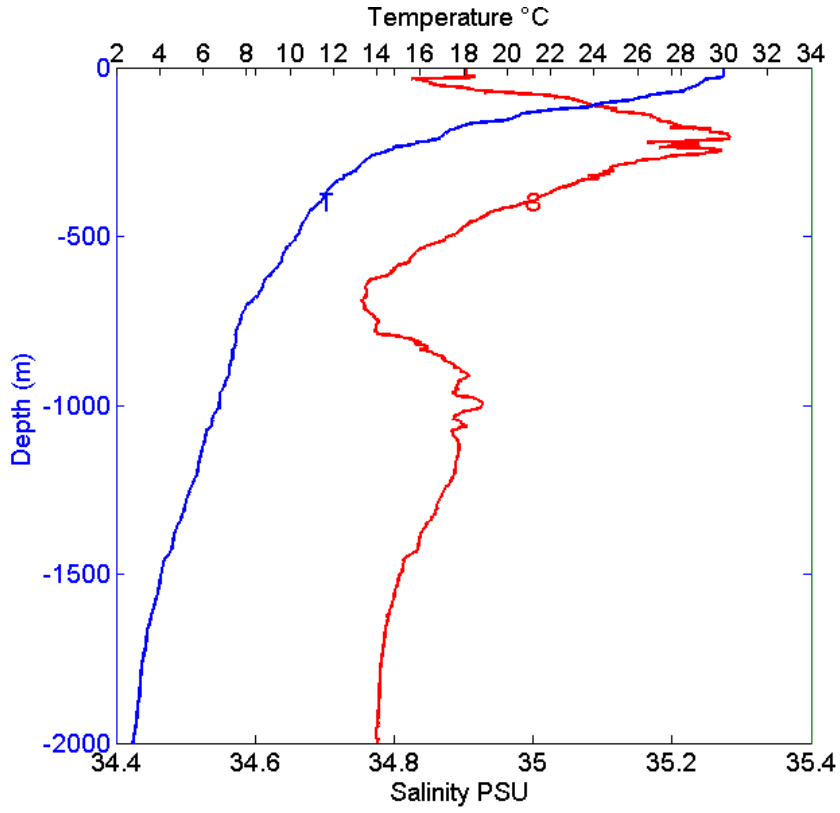

Figure 4(a). *T-S vertical profiles of the deepest station in the sectioned transect 12 ºS. The profiles of Temperature and Salinity are represented by the colours blue and red respectively.*

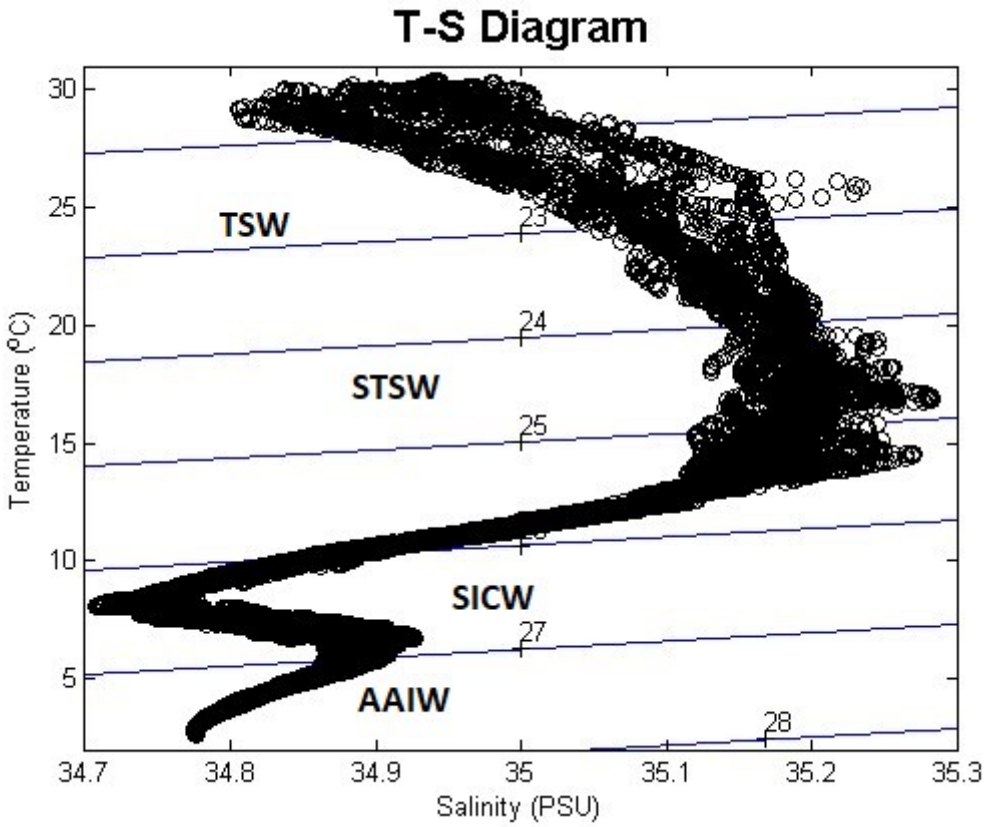

Figure 4(b). *T-S diagram of the water masses of the sectioned transect 12 °S, where: TSW – Tropical Surface Water, STSW - Subtropical Surface Water, SICW - South Indian Central Water and AAIW - Antarctic Intermediate Water.*

4.1.2 Sections of Temperature, Salinity and Sigma-theta

Figures 5(a), 5(b), and 5(c) present the sections of the temperature, salinity, and Sigma-theta parameters for the longitudinal transect, with 200 m as a referential depth, where the parameters vary greatly. The full depth CTD sections are presented in the appendix chapter 8.2.

4.1.1.1 Temperature

Figure 5(a) presents the temperature distribution at the transect, where it is possible to observe typical characteristics of tropical shallow waters with well-observed stratification. The surface temperatures are high up to 30 ºC, with a uniform layer of 28 ºC temperature observed between 20 m and 60m depths. Below this depth, the temperature distribution decreases gradually, with 16 ºC at the reference depth of 200 m.

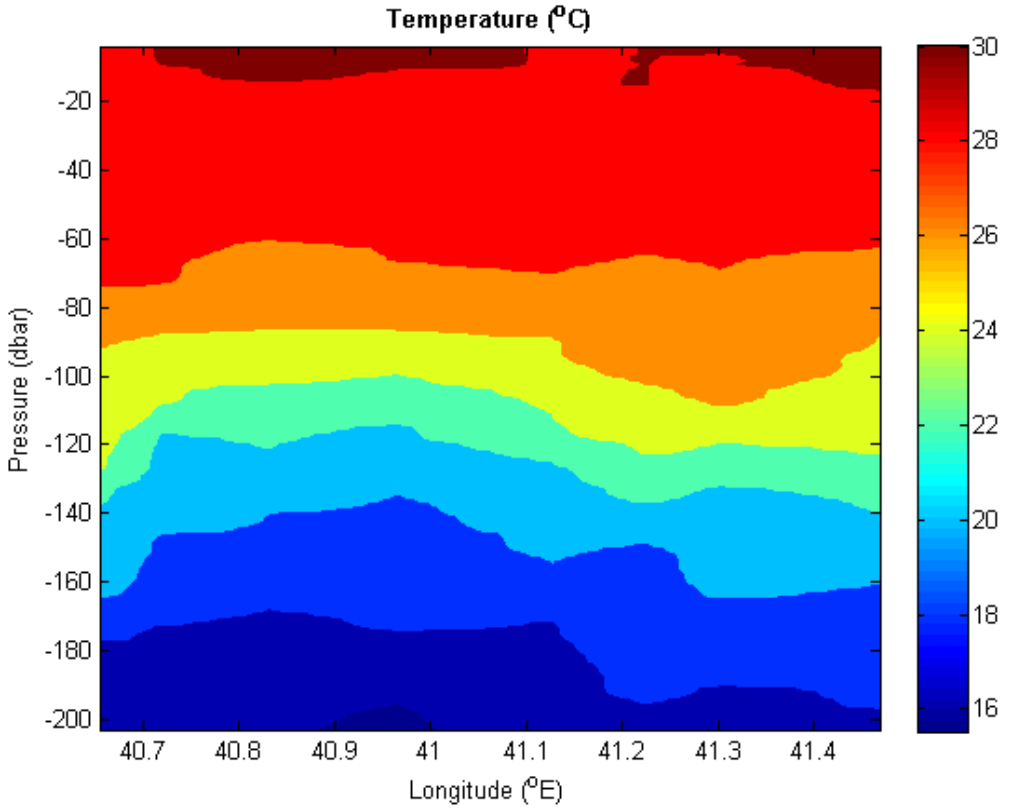

Figure 5(a). *Section of Temperature distribution upper 200 m at the transect 12 ºS.*

4.1.1.2 Salinity

Figure 5(b), presents the salinity distribution at the transect, where at the surface up to 80 m depth is marked by medium salinity values of 34.9 ‰ in most of the transect. It is also possible to observe salinity isolines ranging from 34.7 ‰ to 34.8 ‰ in some specific stations. Below the depth of 80 m, the salinity increases gradually in depth with high salinities up to 35.2 ‰, scattered along the longitudinal section.

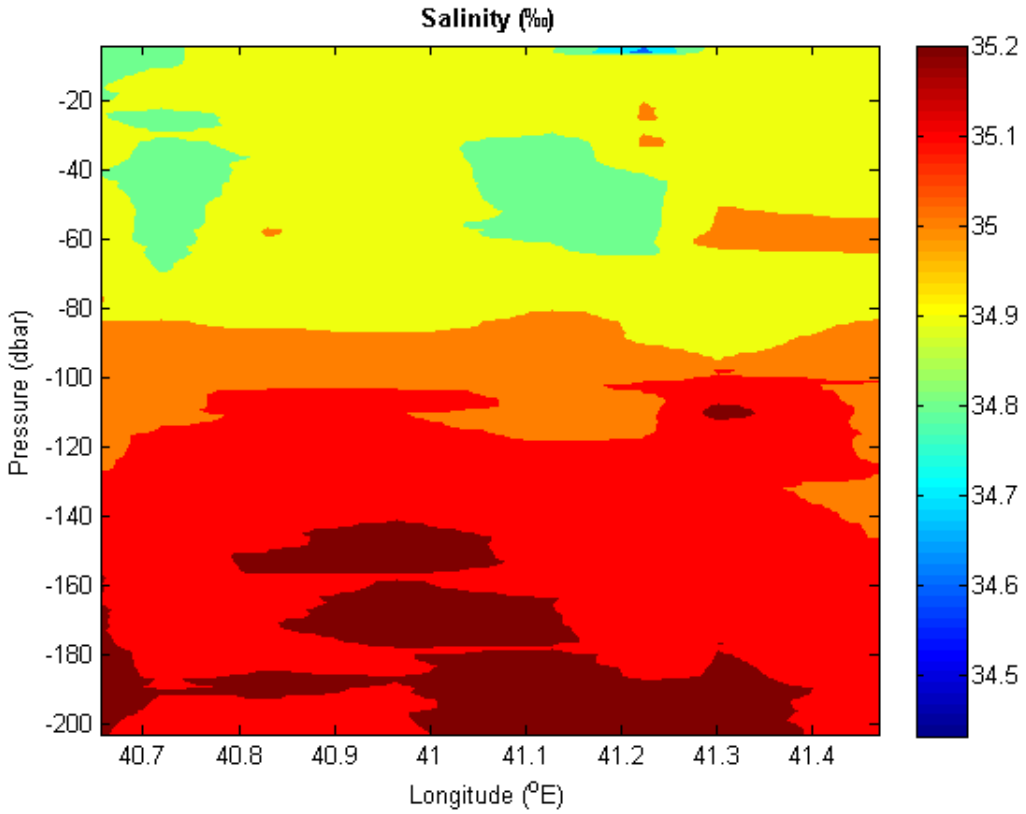

Figure 5(b). *Section of Salinity distribution upper 200 m at the transect 12 °S.*

4.1.1.3 Sigma-theta

Figure 5(c), presents the sigma-theta distribution at the transect, which is the water density calculated considering the pressure equal to zero, and 1000 kg.m^{-3} is subtracted. The density is a function of temperature, it increases with decreasing temperature. It is possible to observe that the sigma-theta profile has an inverse relationship with the temperature profile (see Figure 5a). The lowest values are observed at the surface at up to 80 m depths, ranging from 21.5 kg.m^{-3} to 22.5 kg.m^{-3}. Below the 80 m depth, the values increase gradually along the longitudinal transect, with a maximum of up 25.5 kg.m^{-3} at the reference depth of 200 m.

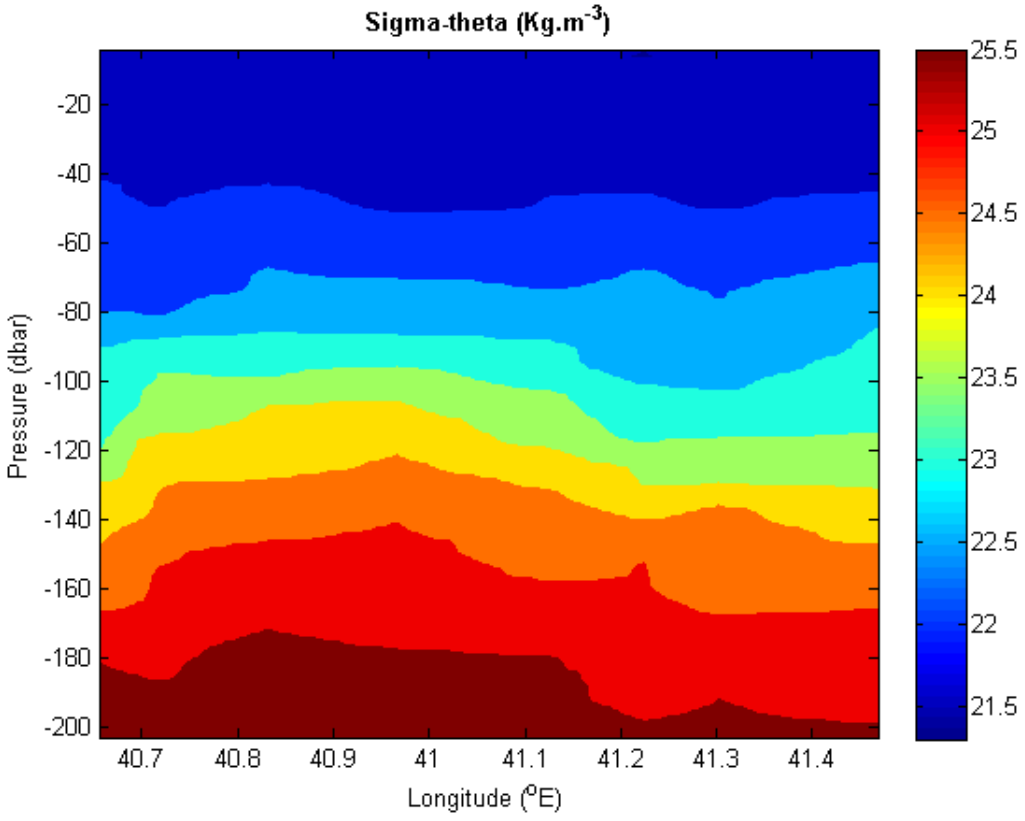

Figure 5(c). *Section of Sigma-theta distribution upper 200 m at the transect 12 °S.*

4.2 Currents

Currents direction and velocity measured by the ADCP and geostrophic currents derived from CTD measurements for the 200 m depth (referential depth), along the transect located between 40.7 ^{o}E and 41.4 ^{o}E, are presented in figures 6, 7(a), 7(b) and 7(c).

Based on the flow pattern of the currents and the bathymetry of the seabed, it is possible to distinguish three subsections along the transect of the ADCP measured currents, presented in Figure 6. The first subsection, along the western tip of the transect to around 500 m isobaths ranging from 40.7 ^{o}E to 40.9 ^{o}E (named as A), the second, 1000 m isobaths between 40.9 ^{o}E and 41.2 ^{o}E (named as subsection B) and the third one 2000 m isobaths between 41.2 ^{o}E and 41.4 ^{o}E (named as subsection C).

In general overview, along subsection A the currents are vertically homogeneous, southwards oriented with velocities around 0.6 m/s. Subsection B presents stronger and mostly south-westwards going currents, with speed of about 1 m/s in the first 150 m, followed by a slight decrease up to 0.6 m/s below this depth. Subsection C shows currents with a differentiated structural variability field, with weak up to 0.2 m/s north-westward going currents in the first 20 m depth, followed by an abrupt intensification to around 0.5 m/s and change in direction to south-eastward along 70 m to 120 m. Below this depth, the currents are relatively weak exhibiting an opposite direction to the Northward.

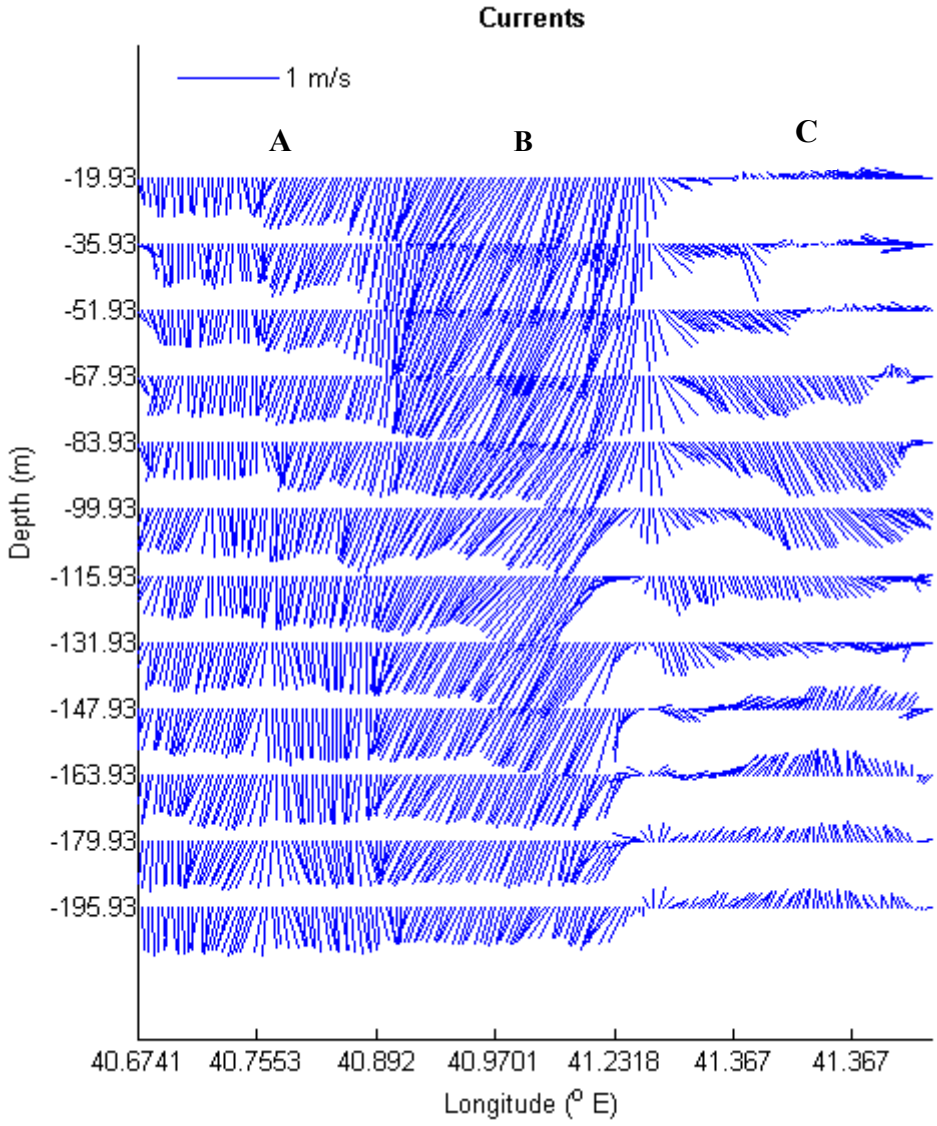

Figure 6. *Currents of each horizontal thin layer of water, the transect was discriminated according to pattern flow and bathymetry isobaths where: Subsection A - 500 m (40.7 ºE - 40.9 ºE), Subsection B - 1000 m (40.9 ºE - 41.2 ºE) and Subsection - 2000 m and over (41.2 ºE - 41.4 ºE).*

Figure 7(a), represents the East velocity component of currents measured by ADCP along the section, where the currents present varying speeds with a westward (negative) and eastward (positive) flowing along the section. The highest speeds (up to 0.6 m/s) intensify from 41 ºE to 41.2 ºE, with a westward flowing mode from the surface to 140 m. The lowest current velocities are found at the coast and the end of the section. The Easterly flowing mode with weak velocities up to 0.2 m/s is observed at the extremities of the section. Null velocity currents are found elsewhere in the transect section mainly on the coast.

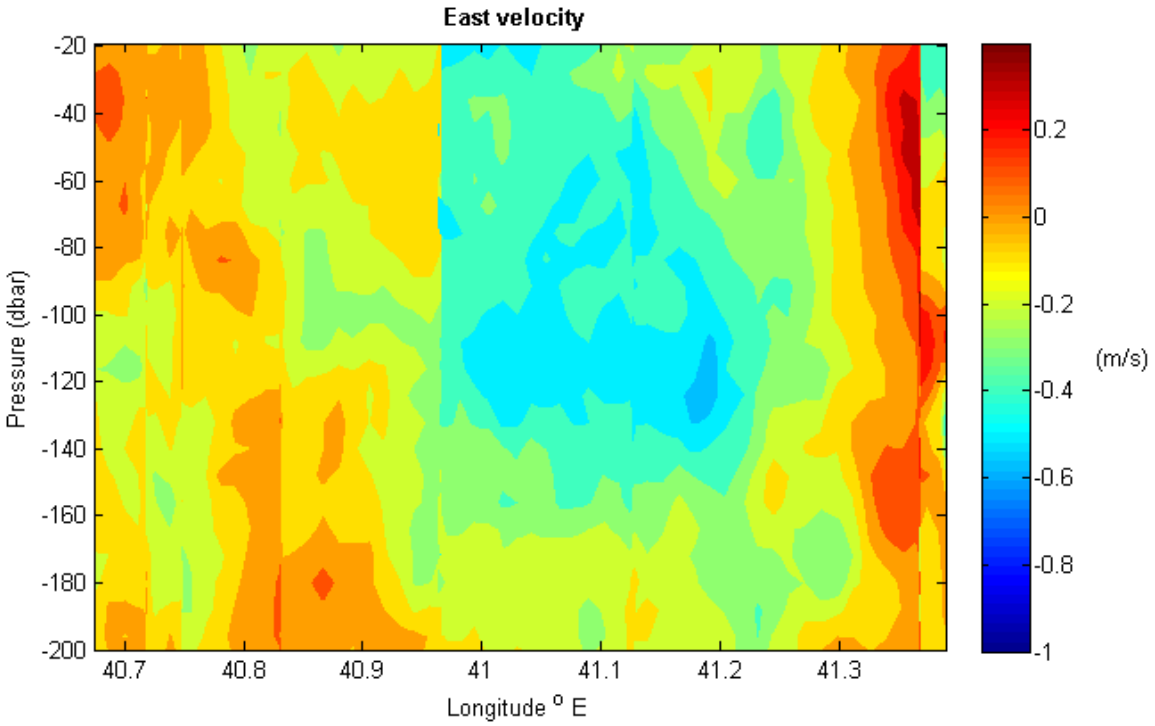

Figure 7(a). *Vertical distribution of the East currents velocity, the positive values indicate the East orientation and the West orientation with the negative values.*

Figure 7(b), represents the North component of currents measured by ADCP along the section, with positive (negative) values corresponding to northwards (southwards) orientation, where a horizontal gradient, can be highlighted, especially in the first 150 m depth.

The mentioned horizontal gradient is characterized by an intensification from about 0.2 m/s south-going currents in the coastal tip of the transect to a maximum of about 1 m/s near 41.3 ^{o}E, followed by a decreasing to close to null in the eastern tip of the transect, suggesting weakness of the north component in that region.

Figure 7(c), represents the current velocities of the calculated geostrophic currents derived from the CTD measurements for the North component. One can visualize that the horizontal gradient has a structural field that tends to resemble that of the current velocities measured by the ADCP (Fig. 7b). Although the northwards going currents at the Eastern tip are relatively evident in Figure 7c, with current velocities higher than 0.2 m/s.

The comparison of the North currents velocities between the currents measured by the ADCP (Fig. 7b), and the calculated geostrophic currents from the CTD (Fig. 7c), indicate that the vertical structure is of the same order of magnitude.

Comparing the two components East and North, it is possible to notice that the North component has much more influence in the current field than the East component, which is justified by the coast topography.

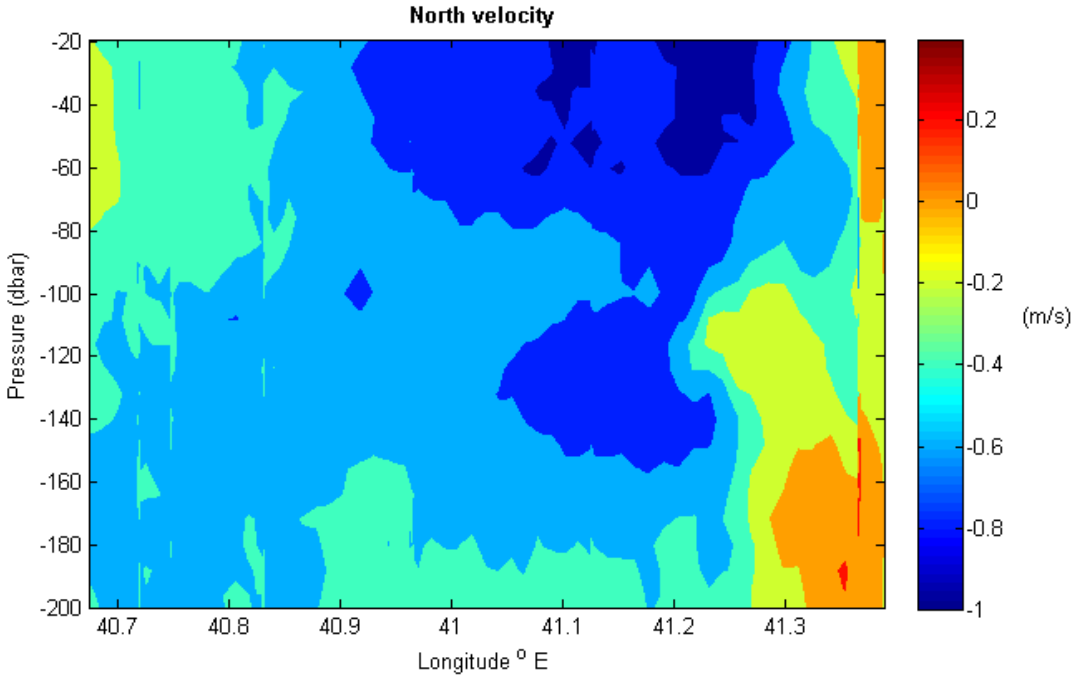

Figure 7(b). *Vertical distribution of the North currents velocity, the positive values indicate the North orientation and the negative values indicate the South orientation.*

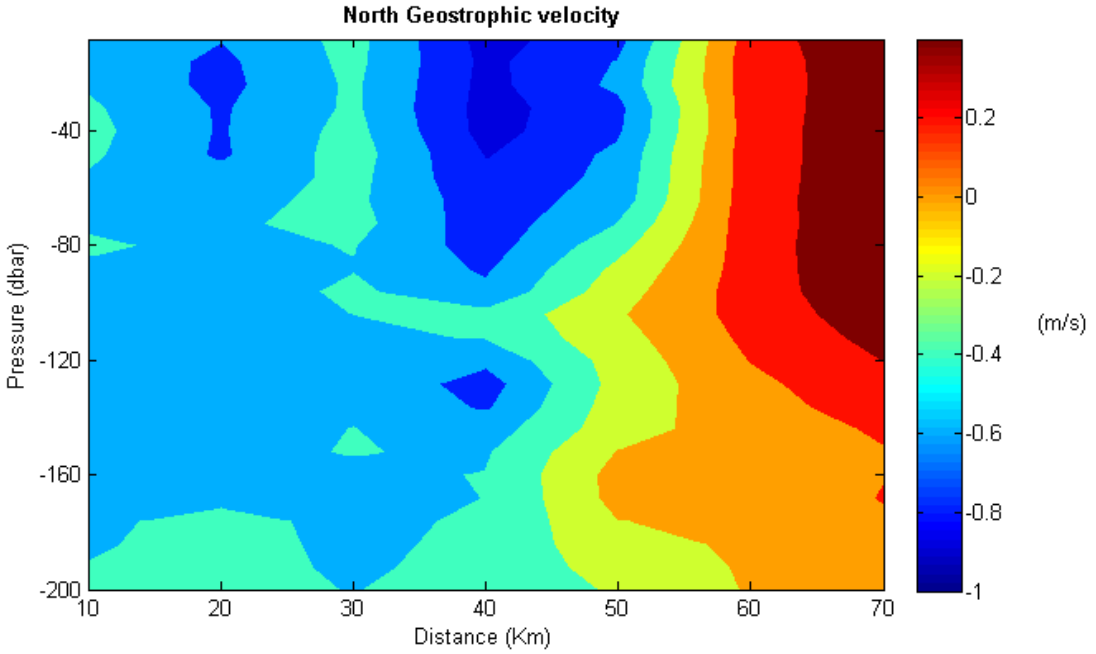

Figure 7(c). *Same as figure (Fig. 7b), but this is related to the velocity of the geostrophic current calculated from CTD measurements and constructed by the ADCP values at 200 m.*

4.4 Geostrophic Currents and Sea Level Anomaly

Figure 8, represents the horizontal fields of the near surface geostrophic currents calculated according equations 4a and 4b, plotted with the SLA corresponding to the average of the two days of current measurements (25th and 26 th, March 2018).

From a general overview, it is possible to visualize that the geostrophic currents have a variety of horizontal structure fields, where between the 12 ºS to around 14 ºS, it is possible to observe strong southwards flowing currents from the coastal tip, which exhibits negative SLA almost 0.1 m. In more seawards 42 ºE the currents are weak with a slightly positive SLA of up to 0.2 m, followed by a strong northwards going currents around 43 ºE - 44 ºE. Close to the Northern tip of the coast of Madagascar, the currents are moderate and a possible anticyclone eddy is formed exhibiting weak currents with a positive SLA of about 0.2 m at 47 ºE. Interestingly at the narrow section of the Channel 16 ºS, strong currents are observed and a possible cyclone eddy is formed with apparent positive SLA > 0.2 m.

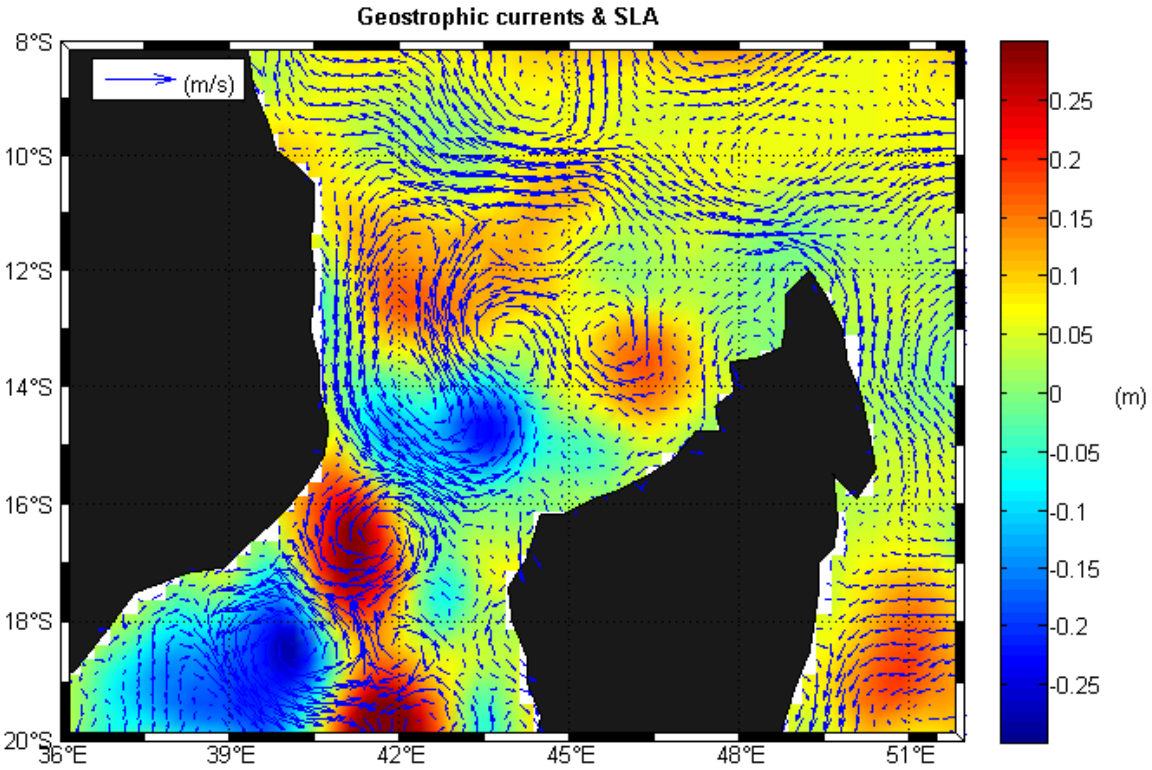

Figure 8. *Geostrophic currents averaged for the two days of measurements with the Sea Level Anomaly for the Northern Mozambique Channel domain.*

5 DISCUSSION

Various technological advances have been applied in several researches to gain a detailed understanding of the dynamics and circulation patterns in the Mozambique Channel in general. Generally, it can be assumed that the observations carried out indicate a high influence of mesoscale turbulence throughout this region, and consequently, the geostrophic response to the sea surface topography.

5.1 ADCP Currents and Altimetry Geostrophic Currents

Comparing the surface velocity along track ADCP and the velocity of the geostrophic current, derived from the satellite Figure 9, one can easily visualize that the two products present a good qualitative agreement for the horizontal field structure of the currents, and at the surface, both products presents a southwards flowing current. Although the two products present currents flowing in the same direction in many parts of the transect (especially on the western side of the coast), there are small differences, most notably the weak northerly current, captured by the ADCP and not by altimetry-based satellite at the extremity of the transect 42 ^{o}E. These discrepancies are most likely related to their different spatial and temporal resolutions, the gridded Sea Surface Height fields: the temporal (daily) or the spatial (0.25^{o}) resolutions. On the other hand, it wasn't possible to consider the ADCP measurements above 20 m depths, since they are affected by greater turbulence due to the ship's movement. Surface currents based on satellite altimetry were also discussed by Ternon et al., (2014), which compared in situ measurements by ADCP and satellite SLA. They pointed to the differences in spatial and temporal resolutions as the cause of the underestimation of satellite measurements.

In recent days, the technology has advanced and the geostrophic velocity field deduced from altimetry has been significantly improved by using multi-mission altimetry products (Ternon et al., 2014). However, despite these improvements, the velocity field remains coarse and underestimated compared with the in-situ measurements, as observed in this study.

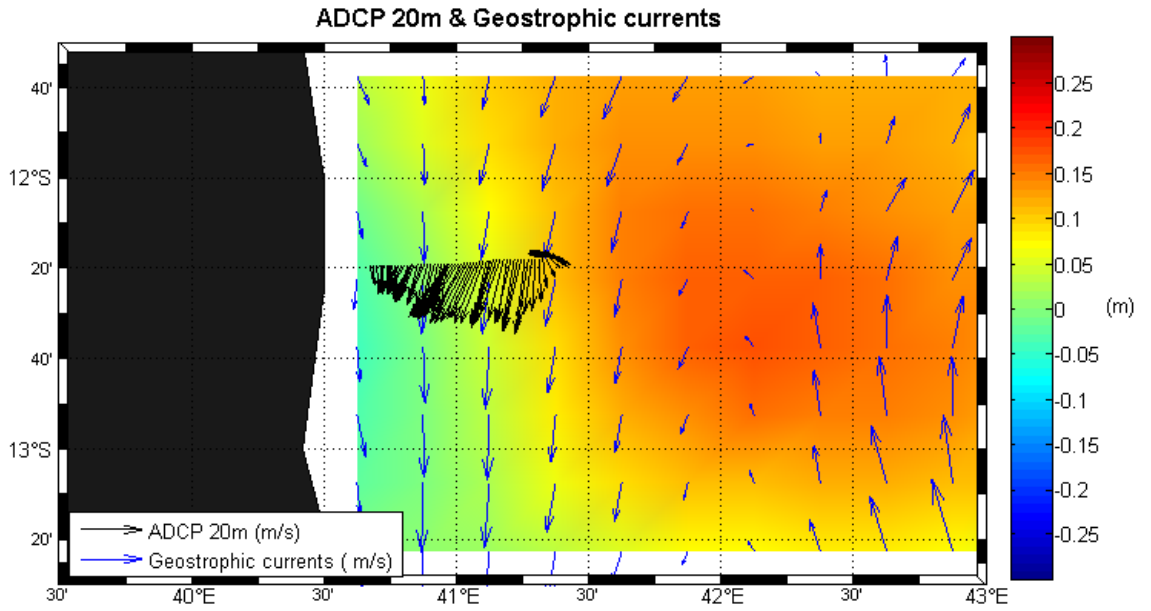

Figure 9. *Geostrophic currents plotted with the ADCP measured currents and the SLA. The black arrows are the ADCP current vectors and the blue are the geostrophic currents vectors.*

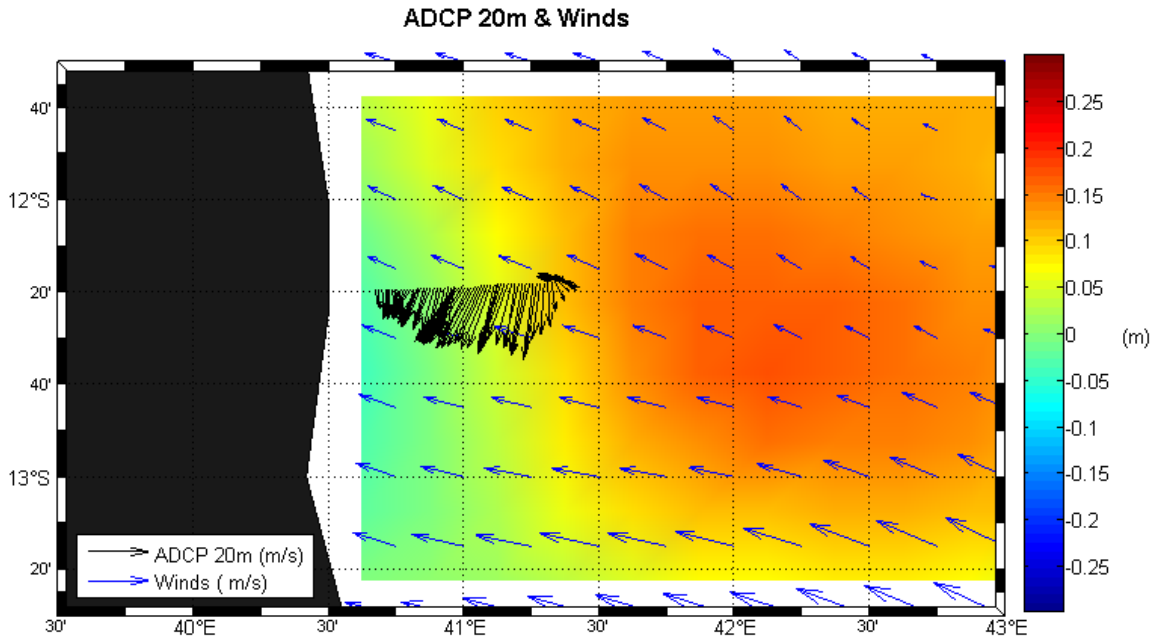

Figure 1. *Wind component plotted with the ADCP measured currents and the SLA. The black arrows are the ADCP current vectors and the blue are winds vectors.*

This study has provided some new insights into the current field structure in the Northern Mozambique Channel, Cabo-Delgado, which is highlighted by the appearance of strong currents of almost 1m/s throughout the water column 200 m, intensifying from the coast into the open sea from subsection A to subsection B as observed in Figure 6, with a southwards (subsection A: 500 m isobaths) and south-westwards (subsection B: 1000 m isobaths). Although this flowing mode of the currents is not observed over the entire longitudinal transect, in more seawards of subsection C (2000 m isobaths) the currents present a varied structure in both depth and direction, displaying weak north-westward currents near the surface (above 20 m) and an abrupt south-eastwards intensification between 70 m and 100 m. Below this depth, the current direction shifts northwards exhibiting weak speeds of about 0.2 m/s.

While the strong south-westwards flowing currents in most of the transect are induced by the SSH gradient, the weak north-westwards currents, near the surface, at around 41.3 ºE are found to be wind-driven, with less influence from the SSH gradient, given that the area is within a high Sea Surface (Fig. 10).

These current structure characteristics of strong southwards currents on the western side and weak northwards currents on the eastern side were previously observed by Lutjeharms et al., (2012), but in the narrow section of the channel along 16 ºS, which means it extends to the Northern Mozambique Channel.

The analysis of SLA (Fig. 8) can help to understand the formation of eddies else-where in the Channel, where an elongated anticyclonic eddy flowing southwards is formed at the section and another one is seen at the northern tip of the Madagascar coast whereas a cyclonic is seen at 16 ºS western of the Mozambique Channel as previously proposed by Sætre, (1985). Such scenarios correspond with the “classical” scheme of eddy formation in the Channel further resulting in the propagation and intensification of anticyclones along the western side of the Mozambique Channel.

The south-westerly propagating currents observed in this study are in concordance with previous findings by Schouten et al., (2003), who associated it with the fundamental pattern of typical variability within the Mozambique Channel dominated by the southward migrating anticyclones as mentioned above.

Although our study was limited to the upper 200 m, we presume that the flowing mode found in this study can be expected in the whole water column of the current as observed by Ullgren et al., (2016), who, using 1000 m moored current meters, registered four events of strong bottom currents up 0.6 m/s flowing south-westwards, where the currents were aligned with the bottom topography along 13 ^{o}S.

It is worth mentioning that, from the perspective of hydrocarbon exploitation in Cabo-Delgado, these speeds of the surface current highlighted in this study and the other previous findings of the bottom currents discussed by Ullgren et al., (2016), can be considered very strong for the safety of offshore operations and eventual environmental issues including oil spill.

6 SUMMARY and CONCLUSIONS

In this present study, we used a combination of different data set products to investigate the current structure and processes that govern the variability and dynamics in the Northern Mozambique Channel, Cabo-Delgado, Quissanga at 12 ^{o}S, namely in-situ ADCP and CTD parameters together with satellite altimeter geostrophic currents.

The main findings can be summarised as follows:

- In a horizontal view, the current structure is identified by 3 different flowing modes: (1) The coastal tip (500 m isobaths) the currents are moderate and vertically homogeneous, with speeds of up to 0.6 m/s; (2) the central part of the section (1000 m isobaths), with very strong currents of up to 1 m/s up to 150 m depth, followed by a slight decrease of up to 0.6 m/s at depths below; (3) the eastern end of the section (2000 m isobaths), presented very weak currents with a north-westwards orientation near the surface (above 50 m depth), followed by a change of direction to the south-eastwards, and an increase in speed of up to 0.5 m/s at depths between 70 m and 100 m. Below this depth, the currents are weak and northwards orientated;

- The strong currents that characterized the most portion of the section are SSH induced with an eventual contribution of the local topography and coastal orientation, however, when the altimetry gradient is low, the wind takes a noticeable role as seen in the eastern of our section

- Both in situ currents measured by the ADCP and the altimetry-based geostrophic currents captured the main structure of the currents in the study area, however, the geostrophic model didn't capture the weak north-westwards going flow driven by the wind because it doesn't consider the wind influence.

These findings elucidate the necessity of delicate and appropriate materials and methods for operations offshore as the FLNG platforms will have to withstand the forces of ocean currents as strong as 1 m/s at a depth of more than 1000 m isobaths, these current velocities presented in this study are very strong and in case of an oil spill can reach faster the coast affecting the coastal ecosystem and consequently human health.

7 References

Backeberg, B. C., & Reason, C. J. C. (2010). A connection between the South Equatorial Current north of Madagascar and Mozambique Channel Eddies. *Geophysical Research Letters*, *37*(4), 1–6. https://doi.org/10.1029/2009GL041950

Breitzke, M., Wiles, E., Krocker, R., Watkeys, M. K., & Jokat, W. (2017). Seafloor morphology in the Mozambique Channel : evidence for long-term persistent bottom-current flow and deep-reaching eddy activity. *Marine Geophysical Research*, *38*(3), 241–269. https://doi.org/10.1007/s11001-017-9322-7

Dimarco, S. F., Chapman, P., Nowlin, W. D., Hacker, P., Donohue, K., Luther, M., Johnson, G. C., & Toole, J. (2002). Volume transport and property distributions of the Mozambique Channe*l*. *49*, 1481–1511.

Donguy, J.-R., and Piton, B. (2005). The Mozambique Channel revisited. *The Missouri Review*, *28*(2), 12–41. https://doi.org/10.1353/mis.2006.0018

Gammelsrød, T. (2008). Oceanography Introductory notes. NOMA MSc Programme in Oceanography Mozambique, Sudan, Norway. University of Bergen.

Halo, I. F. M., (2012). The Mozambique Channel Eddies : Characteristics and Mechanisms of Formation. University of Cape Town, *September*.

Halo, I., Backeberg, B., Penven, P., Ansorge, I., Reason, C., & Ullgren, J. E. (2013). Author ' s Accepted Manuscript Eddy properties in the Mozambique Channel : A comparison between. *Deep-Sea Research Part II*. https://doi.org/10.1016/j.dsr2.2013.10.015

Hancke, L., Roberts, M. J., & Ternon, J. F. (2014). Deep-Sea Research II Surface drifter trajectories highlight flow pathways in the Mozambique Channel. *Deep-Sea Research Part II*, *100*, 27–37. https://doi.org/10.1016/j.dsr2.2013.10.014

Harlander, U., Ridderinkhof, H., Schouten, M. W., & Ruijter, W. P. M. De. (2009). Long-term observations of transport, eddies, and Rossby waves in the Mozambique Channel. *114*(October 2008), 1–15. https://doi.org/10.1029/2008JC004846

Hersbach, H., Bell, B., Berrisford, P., Hirahara, S., Horányi, A., Muñoz-Sabater, J., Nicolas, J., Peubey, C., Radu, R., Schepers, D., Simmons, A., Soci, C., Abdalla, S., Abellan, X., Balsamo, G., Bechtold, P., Biavati, G., Bidlot, J., Bonavita, M., … Thépaut, J. N.

(2020). The ERA5 global reanalysis. *Quarterly Journal of the Royal Meteorological Society*, *146*(730), 1999–2049. https://doi.org/10.1002/qj.3803

Instituto Nacional de Petroleo. (2023, November). Retrieved from http//www.inp.gov.mz

Jornal Nacional. (02.de Julho.2023). Coral Norte sem grandes riscos ao meio ambiente. pp: 3.

Lutjeharms, J. R. E., Biastoch, A., Werf, P. M. Van Der, Ridderinkhof, H., Ruijter, W. P. M. De, Town, C., Africa, S., Albrechts, C., Burg, D., Biastoch, A., & Sciences, M. (2012). On the discontinuous nature of the Mozambique Current. *108*, 1–5.

Miramontes, E., Penven, P., Fierens, R., Droz, L., Toucanne, S., Jorry, S. J., Jouet, G., Pastor, L., Silva Jacinto, R., Gaillot, A., Giraudeau, J., & Raisson, F. (2019). The influence of bottom currents on the Zambezi Valley morphology (Mozambique Channel, SW Indian Ocean): In situ current observations and hydrodynamic modeling. *Marine Geology*, *410*(October 2018), 42–55. https://doi.org/10.1016/j.margeo.2019.01.002

Obura, D. O., Bandeira, S.O., Bodin, N., Burgener, V., Braulik, G., Chassot, E., Gullström, M., Kochzius, M.,Nicoll, M., Osuka, K., Ralison, H.O., Richmond, M., Samoilys, M.A., Scheren, P., Ternon, J-F. (2019). The Northern Mozambique Channel. *World Seas: An Environmental Evaluation*. https://doi.org/10.1016/B978-0-08-100853-9.00003-8 © 2019 Elsevier Ltd. All rights reserved.

Peter, B. N., Ses, S., & Science, F. G. (2010). Surface circulation and transport in the Mozambique Channel. *Geoinformation Science Journal*, Vol. *10*(2), 52–61.

Quartly, G. D., & Srokosz, M. A. (2004). Eddies in the southern Mozambique Channel *$. *51*, 69–83. https://doi.org/10.1016/j.dsr2.2003.03.001

Ridderinkhof, H., & Ruijter, W. P. M. De. (2003). Moored current observations in the Mozambique Channel. *50*, 1933–1955. https://doi.org/10.1016/S0967-0645(03)00041-9

Ruijter, W. P. M. De, Aken, H. M. Van, Beier, E. J., Lutjeharms, J. R. E., Matano, R. P., & Schouten, M. W. (2004). Eddies and dipoles around South Madagascar : formation , pathways and large-scale impact. *51*, 383–400. https://doi.org/10.1016/j.dsr.2003.10.011

Ruijter, W. P. M. De, Ridderinkhof, H., Lutjeharms, J. R. E., Schouten, M. W., & Veth, C. (2002). Observations of the flow in the Mozambique Channel. *29*(10), 3–5.

Sætre, R., and Da Silva, A. (1982). Water masses and circulation of the Mozambican Channel. *Revista de Investigação Pesqueira*, *3*, 3–38.

Sætre, R., and Da Silva, A. (1984). The circulation of the Mozambique Channel, *Deep-Sea Research* , Vol. 31, No. 5, *pp 485 to 508.*

Sætre, R. (1985). Surface currents in the Mozambique channel. *Deep Sea Research Part A. Oceanographic Research Papers*, *32*(12), 1457–1467. http://www.sciencedirect.com/science/article/B757K-48CG4JD-2D/2/08b3364a546111edfcecf722f3e62035

Schouten, P., Leeuwen, V., and Ridderinkhof, H. (2003). Eddies and variability in the Mozambique Channel. *50*, 1987–2003. https://doi.org/10.1016/S0967-0645(03)00042-0

Stewart, R. H. (2008). Introduction To Physical Oceanography. *September*.

Ternon, J. F., Roberts, M. J., Morris, T., Hancke, L., & Backeberg, B. (2014). Deep-Sea Research II In situ measured current structures of the eddy fi eld in the Mozambique Channel. *Deep-Sea Research Part II*, *100*, 10–26. https://doi.org/10.1016/j.dsr2.2013.10.013

Ullgren, J. E., Aken, H. M. Van, Ridderinkhof, H., & Ruijter, W. P. M. De. (2012). Deep-Sea Research I The hydrography of the Mozambique Channel from six years of continuous temperature , salinity , and velocity observations. *Deep-Sea Research Part I*, *69*, 36–50. https://doi.org/10.1016/j.dsr.2012.07.003

Ullgren, J. E., André, E., Gammelsrød, T., & Hoguane, A. M. (2016). Observations of strong ocean current events offshore Pemba , Northern Mozambique. *8778*(July). https://doi.org/10.1080/1755876X.2016.1204172

van der Werf, P. M., van Leeuwen P. J., Ridderinkhof, H., and de Ruijter W. P. M. (2010). Comparison between observations and models of the Mozambique Channel transport: Seasonal cycle and eddy frequencies. *Journal of Geophysical Research*, Vol. 115, C02002, doi:10.1029/2009JC005633

Vassele, V. J. (2010). Eddy structure and dynamics in the Northern Mozambique Channel. Master's Thesis, Bergen University

8 Appendixes

In this chapter we present the step-by-step of processing in the CODAS platform the ADCP and the main physical parameters of the deep CTD sections down.

8.1 ADCP Processing Overview (https://currents.soest.hawaii.edu/)

There are at least four necessary processing steps for ADCP data which are performed by (or made possible) by the CODAS routines.

First: An **ocean reference layer** is used to remove the ship's speed from the measured velocities. By assuming the ocean reference layer is relatively smooth, positions can be nudged to smooth the ship's velocity, which directly results in the smooth reference layer velocity. This was more important when fixes were rare or jumpy (such as with LORAN) or dithered (such as SA GPS signals before 2001).

Second: An **accurate heading** is required. A GPS-derived heading source such as Ashtech, POSMV, or Sea path) may provide a more accurate (though often less reliable) heading source than a gyro. Routines are in place for ping data and UHDAS data to correct the gyro heading with the GPS-derived heading, using a quality-controlled difference in headings. An example is available for VmDAS data. Gyro headings may be reliable but they can vary with oscillations of several degrees over several hours, thus creating spurious fluctuations in the ocean velocity that resemble "eddies", but which are soley the result of cross-track velocity errors (from the associated gyro heading errors).

Third: Calibration routines are available to estimate the heading misalignment from either "bottom track" or "water track" data. Water track calibration routines use sudden accelerations (such as stopping and starting of the ship when doing station-work) to derive an estimate if the heading misalignment. For a ship travelling at 10 kts, a 1-degree heading error results in a 10 cm/s cross-track velocity error. It is critical that the misalignment be accounted for if one is to avoid cross-track biases in the velocities. Additional calibration routines estimate the horizontal offset between the ADCP and the GPS used to determine ship's speed. An offset of more than a few meters can cause artifacts when the ship turns.

Fourth: Bad data must be edited out prior to use. It is best if the single-ping data can be edited prior to averaging (to screen out interference from other instruments, bubbles, and some

kinds of underway bias). Once the data are averaged and the above steps are applied, it is still often necessary to further edit the data (i.e. remove in-port data or velocities below the bottom). To some extent this can be automated but for final processing, a person must visually inspect all the averages from a dataset.

8.2 CTD Deep Sections

This section presents vertical profiles of Temperature, Salinity and Density at all depths of the CTD casts for the longitudinal transect section, represented in Figures 11(a), 11(b) and 11(c). The stations do not have the same depths, ranging from at least 200m to 2000m. In the main work, we present results corresponding to 200m as the reference depth in all stations. The highest temperatures of up to 30 ºC are observed at the surface and gradually decrease to a minimum of 2 ºC at 2000m. On the other hand, the salinity profile does not allow us to observe great variations in the distribution of salinity, ranging from a maximum of 35.2 ‰ to a minimum of 34.7‰. The density distribution profile shows an increasing variation with lower values at the surface of 22 kg/m3 which gradually increases to 27 kg/m3 at the bottom at 2000m.

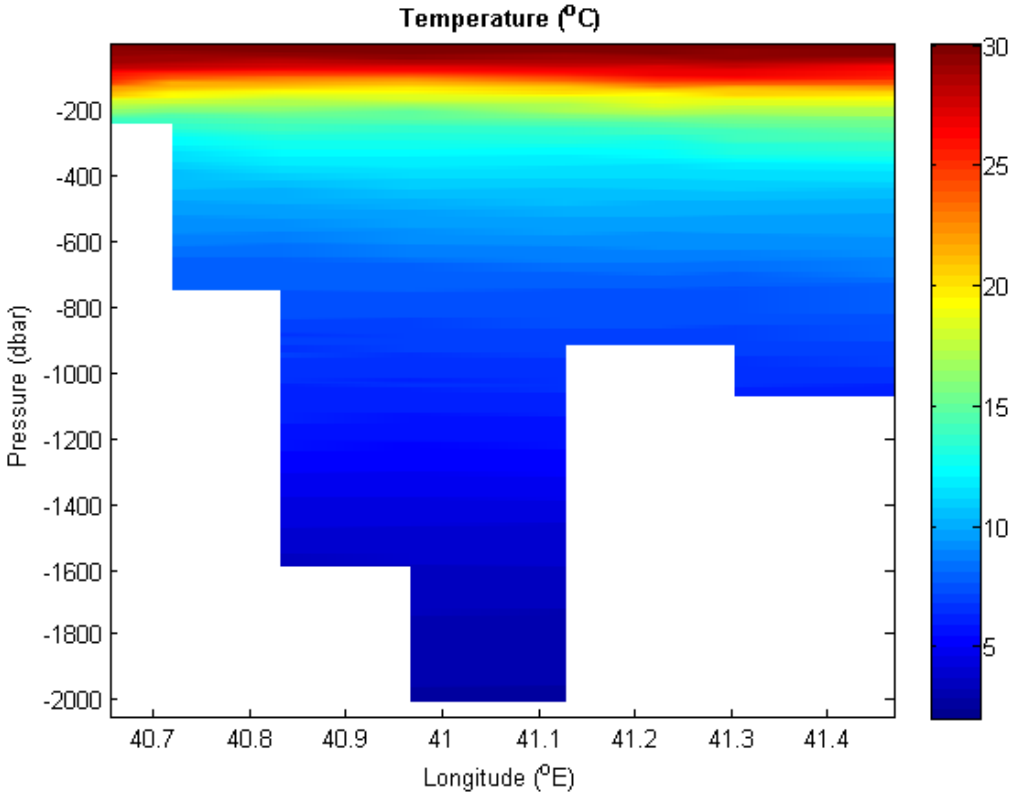

Figure 11(a). *Distribution of temperature at section.*

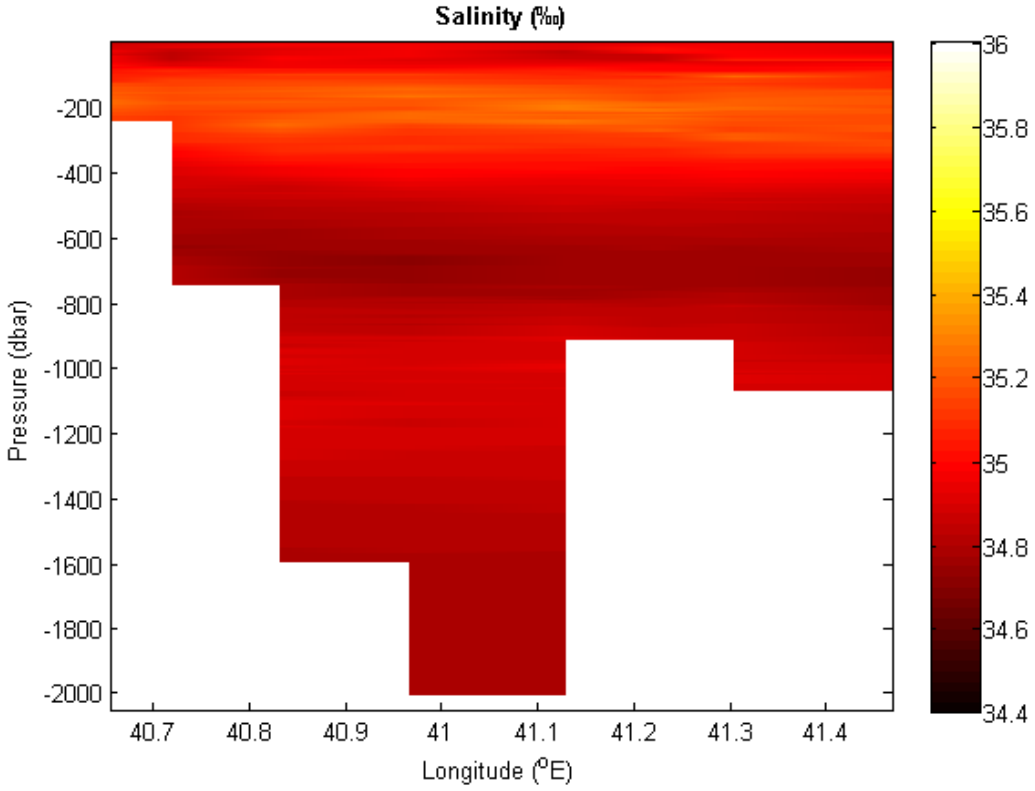

Figure 11(b). *Distribution of salinity at section.*

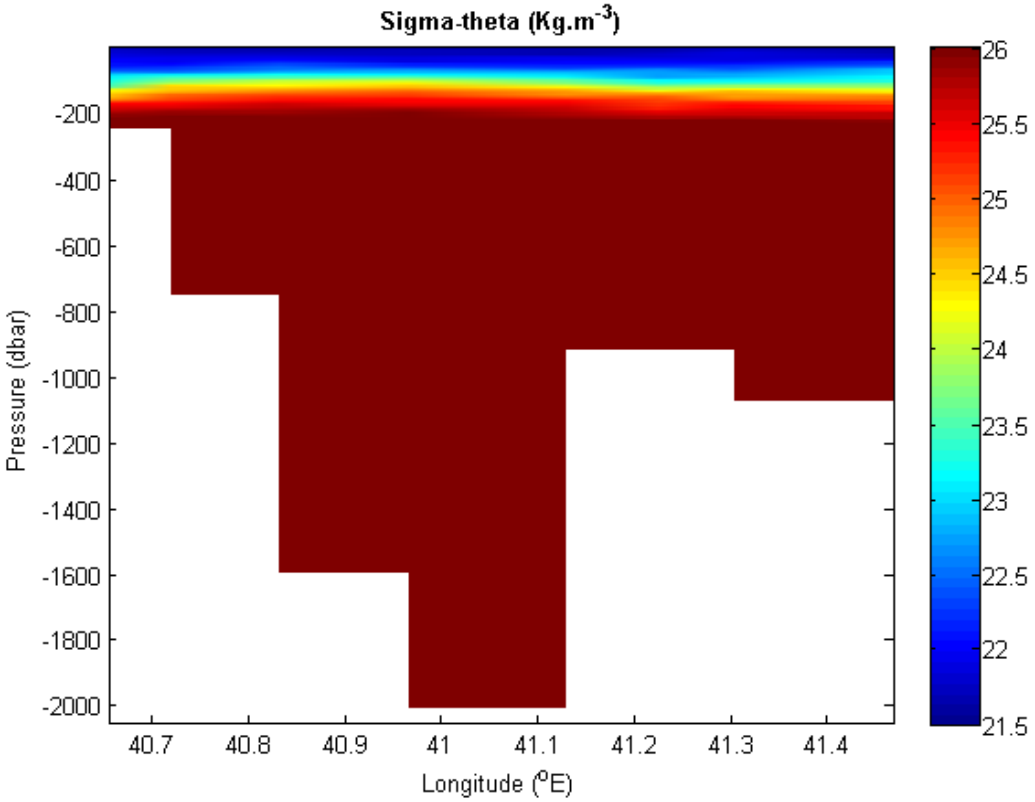

Figure 11(c). *Distribution of density at section.*